Structure–Property Relationship

DOI: 10.1002/anie.201209151

$Cs_2B_4SiO_9$: A Deep-Ultraviolet Nonlinear Optical Crystal**

Hongping Wu, Hongwei Yu, Shilie Pan, Zhenjun Huang, Zhihua Yang, Xin Su, and Kenneth R. Poeppelmeier**

The generation of deep-ultraviolet (UV) coherent light from nonlinear optical (NLO) materials[1–4] as one of the most promising resource, has become a topic of intensive study because of its important applications in a broad range of fields, such as semiconductor photolithography, laser micromachining, photochemical synthesis, and material processing. They are able to shorten the wavelength of light by a factor of two (or doubling the frequency), based on the process of second-harmonic generation (SHG), which occurs only when a centrosymmetric symmetry operation is absent in a crystal. However, for a noncentrosymmetric (NCS) crystal to be used as a nonlinear optical material the essential crystal property requirements are that the crystals possess a large NLO response, wide transparent window, suitable birefringence for phase-matching, good mechanical strength, and chemical stability.[4,5]

After continuous efforts over several decades, many NCS compounds were obtained by incorporating functional borate structure units, such as B_3O_6 and B_3O_7. β-BaB_2O_4 (BBO)[6] and LiB_3O_5 (LBO)[7] are the most advanced NLO materials, which have widely been used as optoelectronic devices. However, to date, $KBe_2BO_3F_2$ (KBBF)[8,9] is the only material that can generate coherent light wavelengths below 200 nm by direct SHG, which makes KBBF a research hotspot. Unfortunately, the KBBF crystal is very difficult to grow in thickness owing to the growth habit of the layer, which severely limits the coherent light output power. Thus, finding the optimal composition that is facile to synthesize, yields large single crystals, and simultaneously satisfies the NLO requirements has attracted considerable attention.[10,11]

The presence of large NLO coefficients in a structure is usually in contradiction with wide band gaps in one compound. For instance, the structural units in the known compounds are second-order Jahn–Teller (SOJT) polar displacements of d^0 metal centers (e.g., Ti^{4+}, Ta^{5+}, and Mo^{6+}),[12–14] anionic groups with stereochemically active lone pairs (e.g., $[IO_3]^-$ and $[TeO_x]^{n-}$),[15,16] or polar chalcogenide units (e.g. $[AsS_3]^{3-}$, $[SbS_3]^{3-}$, and $[TeS_3]^{2-}$),[17] which combine with diverse other functional building units to produce materials with large NLO coefficients, for example, $Cd_4BiO(BO_3)_3$ ($6\times$KDP),[18] $Pb_2B_5O_9I$ ($13.5\times$KDP),[19] and $Ba_{23}Ga_8Sb_2S_{38}$ ($22\times AgGaS_2$).[20] However, the structural units produce an unwanted effect—the UV absorption edge shifts toward the red region, making them less suitable for the deep-UV applications. It is necessary to create the subtle balance of above-mentioned conflicting factors so as to search for the new deep-UV NLO crystals with excellent comprehensive performances.

To circumvent the wide absorption window requirement, basic structural units having excitation energies near the UV region are necessary. Such units are BO_3, BO_4, SiO_4, and PO_4.[6,7,21] A compound $Rb_2Be_2Si_2O_7$[22] was ever expected to be a substitution for KBBF owing to its similar structure characteristics with KBBF and without the layer habit. But, the weak SHG response of $Rb_2Be_2Si_2O_7$ makes the substitution end in naught. However, the borosilicate may be a potential candidate for a deep-UV NLO crystal since the B–O groups are well-known NLO-active groups. Especially in the B-rich borosilicate, the B–O basic units can condense to form large B–O groups. The relative large B–O groups are more flexible than a single SiO_4 tetrahedron. Therefore, when the large B–O groups are connected with SiO_4 tetrahedra to form a three-dimensional (3D) framework, they can easily be pulled to generate large distortions. The large distortions of B–O groups will favor a large SHG response when the inversion symmetry is absent in the crystal. In addition, it is also reported that the size and charge of the cations have influence on the macroscopic NLO properties.[23] Therefore, we choose cations with a large ion radius in alkali-metal systems, which are susceptible to polarization and UV light transmission.[24,25] Thus, a novel borosilicate, $Cs_2B_4SiO_9$ was synthesized. $Cs_2B_4SiO_9$ has an about 4.6 times larger powder SHG response relative to KH_2PO_4 (KDP), which is the strongest among the borosilicates to date, and is phase-matchable. In addition, it is worth noting that $Cs_2B_4SiO_9$ exhibits a short UV cutoff edge (below 190 nm). These results indicate that the $Cs_2B_4SiO_9$ crystal may be a promising NLO material in the deep-UV region and B-rich borosilicate may be a new field for the study of deep-UV NLO materials, for which, to the best of our knowledge, there are no reports about NLO properties.

Single crystals of $Cs_2B_4SiO_9$ were grown from the high-temperature solution using Cs_2CO_3 as the flux system. The crystal structure was solved with SHELXS-97 by a direct

[*] H. Wu, H. Yu, Prof. S. Pan, Z. Huang, Z. Yang, X. Su
Xinjiang Key Laboratory of Electronic Information Materials and Devices, Xinjiang Technical Institute of Physics & Chemistry, Chinese Academy of Sciences
40-1 South Beijing Road, Urumqi 830011 (China)
E-mail: slpan@ms.xjb.ac.cn
Prof. K. R. Poeppelmeier
Department of Chemistry, Northwestern University
2145 Sheridan Road, Evanston, IL 60208-3131 (USA)
E-mail: krp@northwestern.edu

[**] This work was supported by the "National Natural Science Foundation of China" (Grant Nos. 21201176, U1129301, 51172277, 21101168), the National Key Basic Research Program of China (Grant No.2012CB626803).

Supporting information for this article is available on the WWW under http://dx.doi.org/10.1002/anie.201209151.

method[26] and refined using SHELXL-97. During the refinement, it was found that the O1 atom has a large thermal factor, either indicating diffuse positioned atoms or site deficiencies. When refined with the deficiency model, the results showed an O1 site with 50% occupancy and became reasonable when refined together with the fractional occupancy. This occupancy converges better R values, reasonable temperature factors, and a charge-balanced formula. The fractional occupancy of some sites in the crystal structure is observed in other works.[20,27] $Cs_2B_4SiO_9$[28] crystallizes in a NCS tetragonal space group $I\bar{4}$ that is neither chiral nor polar. In the asymmetric unit, each Si and B atom occupies one crystallographically unique position and there are two unique Cs and three unique O positions. $Cs_2B_4SiO_9$ exhibits the framework structure formed from two main units (Figure 1a): First, a new FBB [B_4O_{10}] is observed in Figure 1b (when 50% of the O1 sites are not occupied, the FBB will be

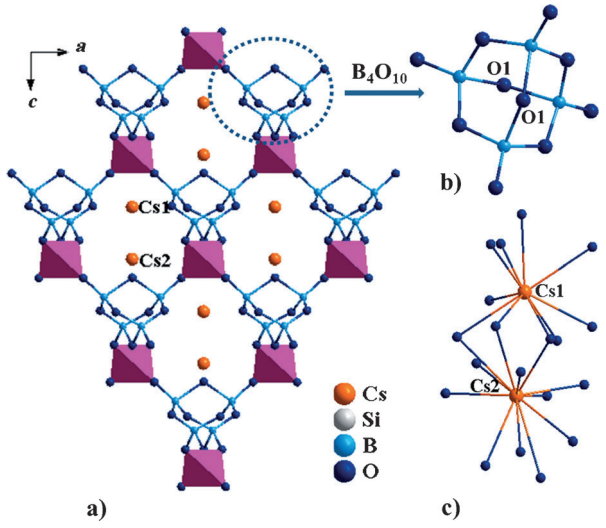

Figure 1. a) The 3D framework of $Cs_2B_4SiO_9$ with Cs–O bonds omitted for clarity viewing along the *b*-axis with b) [B_4O_{10}] group and c) the coordination environment of the Cs atoms (SiO_4 group, rose).

changed to a [B_4O_8] group). The B_4O_{10} groups are connected with neighboring SiO_4 tetrahedra through their terminal O atoms to form a 3D network with tunnels pointing along the *b* axis. The second main unit is the coordination environment of two Cs atoms which fill the tunnels and are linked by oxygen atoms (Figure 1c). The Cs1 atom was coordinated by ten oxygen atoms with Cs–O bond lengths ranging from 3.150(2) to 3.324(5) Å. The Cs2 atom is 12-coordinated by oxygen atoms, and the Cs–O bonds vary from 3.221(3) to 3.547(2) Å (see the Supporting Information).

The B/Si molar ratio of the $Cs_2B_4SiO_9$ structure is 4; the large B/Si ratio makes it possible that the basic BO_4 units condense to B_4O_{10} groups. The relative large B_4O_{10} groups are more flexible than a single SiO_4 tetrahedron, when the B_4O_{10} groups are connected with rigid SiO_4 tetrahedra to form a 3D framework. Therefore, the B_4O_{10} groups can easily be pulled to generate large distortions. As seen in the structure, the B–O bond lengths in the BO_4 units vary from 1.396(5) to 1.671(9) Å (see the Supporting Information). Large distortions in the BO_4 units have been observed in known borates.[29] Neumair et al. classified the BO_4 units with the long B–O bond distance as an intermediate state between a planar BO_3 group and a BO_4 tetrahedron, and regarded them as a superposition of statically or dynamically disordered moieties.[29a] In $Cs_2B_4SiO_9$, owing to the fractional occupancy of the O1 sites, there are BO_3 triangles and BO_4 tetrahedra in the crystal structure, which might be regarded as the statically or dynamically disordered moieties. Therefore, a long B–O bond distance can be accepted. The fractional occupancy of the O1 sites can be further confirmed by IR and Raman spectra. Since the O1 sites are partly occupied, there will be the absorption peaks of BO_4 and also of BO_3 groups. In the IR spectrum (see the Supporting Information),[30] the strong peaks at 1406, 1354, 1298, and 907 cm^{-1} are attributed to the asymmetric and the symmetric stretching of BO_3. The peaks at 1028 and 792 cm^{-1} are attributed to the asymmetric and the symmetric stretching of BO_4. The peaks at 728 and 651 cm^{-1} belong to the out-of-plane bending of BO_3. The peaks at 606 and 523 cm^{-1} are attributed to the bending of BO_3 and BO_4. The peak at 453 cm^{-1} belongs to the bending of BO_4. In the Raman spectrum (see the Supporting Information), Raman-active modes of BO_3 and BO_4 have also been observed.[29a,31] The bands in the range of 1200–1450 cm^{-1} normally correspond to BO_3 groups. The bands at 1112, 1056, 788, 741, and 728 cm^{-1} are attributed to the asymmetric and the symmetric stretching of BO_4. The bands in the range of 969–903 cm^{-1} correspond to the symmetric stretching of BO_3. The bands at 616 and 566 cm^{-1} are attributed to the bending of BO_3 and BO_4. The bands in the range of 486–423 cm^{-1} correspond to the bending of BO_4. These all suggest that the fractional occupancy at the O1 site is reasonable.

The results of bond valence calculations[32] (Cs, 0.89–1.21; Si, 4.06; B, 2.96) indicate that the Cs, Si, and B atoms are in oxidation states of +1, +4, and +3, respectively.[33]

The inductively coupled plasma elemental analysis of $Cs_2B_4SiO_9$ was measured using a Varian Vita-Pro CCD simultaneous inductively coupled plasma-optical emission spectrometer. The calculated analysis for $Cs_2B_4SiO_9$ is: Cs, 55.24; B, 8.99; Si, 5.84. Found: Cs, 55.71; B, 8.85; Si, 5.82. The obtained composition agrees well with the chemical formula determined by single-crystal X-ray diffraction (XRD).

The solid samples of $Cs_2B_4SiO_9$ were synthesized by solid-state reaction techniques, and the powder XRD patterns of the as-synthesized samples show good agreement with the calculated one derived from single-crystal data (see the Supporting Information). The UV/Vis–IR diffuse reflectance spectrum indicates that the UV cutoff edge is lower than 190 nm (Figure 2a). These make $Cs_2B_4SiO_9$ a promising deep-UV NLO crystal.

The thermal behavior of $Cs_2B_4SiO_9$ is measured ranging from 25 to 1200 °C. There is one endothermic peak at 869 °C in the differential scanning calorimetry (DSC) curve, along with weight loss on the thermogravimetry (TG) curve (Figure 2b). To furthermore confirm the thermal behavior of $Cs_2B_4SiO_9$, the solid samples of $Cs_2B_4SiO_9$ from 800 to 860 °C are confirmed by powder XRD, the results show good agreement with the calculated results derived from single-

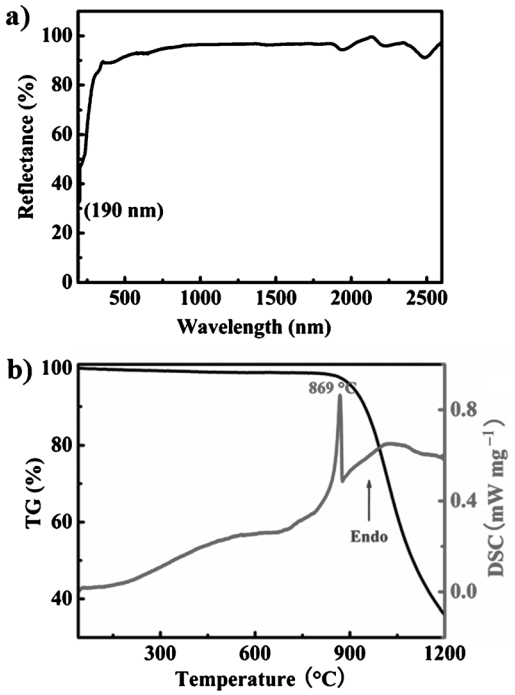

Figure 2. a) UV/Vis–IR diffuse reflectance spectrum of $Cs_2B_4SiO_9$. b) Thermogravimetry (TG) and differential scanning calorimetry (DSC) curves of $Cs_2B_4SiO_9$.

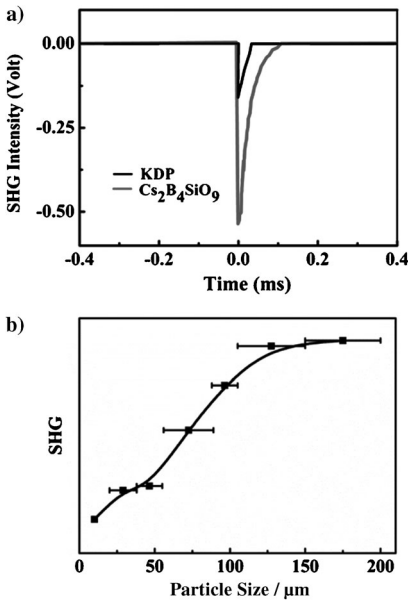

Figure 3. SHG intensities of $Cs_2B_4SiO_9$ with commercial KDP as a reference: a) Oscilloscope traces for the powder of KDP and $Cs_2B_4SiO_9$ and b) phase-matching curve for $Cs_2B_4SiO_9$. (The solid curve drawn is to guide the eye and is not a curve fitted to the data.)

crystal data, whereas a higher temperature (880 °C; 2 h) leads to melting. These characters suggest that $Cs_2B_4SiO_9$ melts at 869 °C, along with volatilization.

$Cs_2B_4SiO_9$ is a NCS compound, the NLO property of which should be studied. We measure the powder SHG intensity using a Q-switched Nd:YAG solid-state laser. $Cs_2B_4SiO_9$ exhibits a 4.6 times larger SHG response relative to commercial KDP at the same particle size of 105–150 μm (Figure 3a), which is the strongest SHG response in a borosilicate system, and it is type-I phase-matchable according to the Kurtz–Perry rule (Figure 3b).[34] And the SHG response of $Cs_2B_4SiO_9$ is stronger than those of the universally used crystals LBO (3 × KDP) and CsB_3O_5 (CBO; 2.7 × KDP).

Where does the enhanced SHG response originate from? It is well-known that the property of the material is governed by its crystal structure.[35,36] For the SHG response, it mainly depends on the distortion of the structure when the compound is NCS.[37] In the structure of $Cs_2B_4SiO_9$, there are three kinds of building units: SiO_4 tetrahedra, B_4O_{10} groups, and CsOn ($n = 10$, 12) polyhedra. As described above, the SiO_4 tetrahedra are rigid and do not contribute to the SHG response. They mainly play a role as nodes to connect the B_4O_{10} groups to form a 3D network. Four distorted BO_4 form the B_4O_{10} groups, which are in-phase aligned in the neighborhood layers. The B–O framework is composed of A^1 repeating units (Figure 4). The analysis indicates that the in-phase alignment of the B–O units, A^1A^1, and the large distortions in the BO_4 tetrahedra have large influence on the SHG response of $Cs_2B_4SiO_9$. Cs^+ cations are readily polarized because of their large size. Therefore, they will also have some contribution to the SHG response.

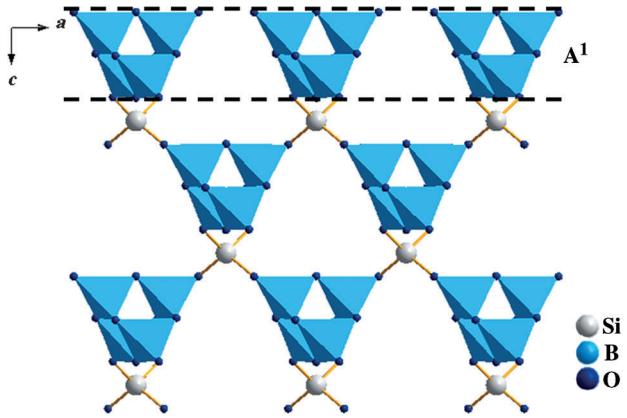

Figure 4. The alignment of B–O units (BO_4 group, light blue).

To further understand the contribution to the SHG response of the building units in $Cs_2B_4SiO_9$, we compute the local dipole moments of the BO_4 tetrahedron and the $Cs1O_{10}$ and $Cs2O_{12}$ polyhedra using a bond-valence approach (Table 1).[38,39] We found that the local dipole moment of the BO_4 tetrahedra in $Cs_2B_4SiO_9$ is 7.44 Debye, which is much larger than that of other reported materials (0.005–0.727 Debye).[40] They are also larger than those of $Cs1O_{10}$

Table 1: The direction and magnitude (in Debye) of the polyhedral dipole moments for $Cs_2B_4SiO_9$.

Species		*x*(*a*)	*y*(*b*)	*z*(*c*)	Magnitude
$Cs_2B_4SiO_9$	$Cs1O_{10}$	0	0	0	0
	$Cs2O_{12}$	−0.78	−1.88	−2.52	3.24
	$B1O_4$	1.48	6.27	3.72	7.44

and $Cs2O_{12}$ polyhedra (0 and 3.24 Debye, respectively). Therefore, we can conclude that the large SHG response of $Cs_2B_4SiO_9$ mainly originates from the large distortions of the BO_4 tetrahedra in the B_4O_{10} groups and $Cs2O_{12}$ polyhedra.

The electronic structure was studied by first-principle calculations. The band structure (see the Supporting Information) reveals that $Cs_2B_4SiO_9$ is an indirect gap compound with a band gap of 4.92 eV, which is comprehensibly smaller than the experimental one of 5.21 eV—a well-known artifact of the DFT functional.[41] Figure S5 (see the Supporting Information) shows the partial densities of states (DOS) and the total DOS. Since the optical properties of a crystal in the visible and UV spectrum are mainly determined by the states close to the band gap,[42] we carefully analyze the upper region of the valence band (VB) and the bottom of the conduction band (CB), the VBs and CBs near the band gap are composed of the O 2p, B 2p, and Cs 6s orbitals, respectively, which could contribute to the greater optical transition matrix elements.

In conclusion, a new B-rich borosilicate, $Cs_2B_4SiO_9$ has been synthesized and characterized. It exhibits the strongest SHG response among borosilicates to date, which is about 4.6 times that of KDP and originates mainly from the distorted BO_4 units and $Cs2O_{12}$ polyhedra. $Cs_2B_4SiO_9$ exhibits a short UV cutoff edge below 190 nm. These properties make $Cs_2B_4SiO_9$ a potential deep-UV NLO crystal. More importantly, $Cs_2B_4SiO_9$ represents a new kind of B-rich borosilicate, and opens a window for the study of deep UV NLO materials.

Experimental Section

Single crystals of $Cs_2B_4SiO_9$ were grown from a high-temperature solution using Cs_2CO_3 as the flux system. This solution was prepared in a platinum crucible after melting the mixture of Cs_2CO_3, H_3BO_3, and SiO_2 with molar ratio of 2:4:1. The Pt crucible, which was placed in the center of a vertical, programmable temperature furnace, was heated to 750 °C, held at this temperature for 10 h, and then quickly cooled to the initial crystallization temperature. The temperature was further decreased to 600 °C at a rate of 2 °C h^{-1}, then allowed to cool to room temperature after the furnace was turned off. Transparent and colorless $Cs_2B_4SiO_9$ crystals were found.

Diffuse reflectance spectra for $Cs_2B_4SiO_9$ samples were measured from 190 to 2600 nm using a Shimadzu SolidSpec-3700DUV spectrophotometer equipped with an integrating sphere attachment.

The study of the thermal behavior of $Cs_2B_4SiO_9$ was carried out on a NETZSCH STA 449C simultaneous analyzer under static air. The sample and reference (Al_2O_3) were enclosed in Pt crucibles, and heated from room temperature to 1200 °C at a rate of 10 °C min^{-1} in flowing nitrogen gas.

An infrared spectrum was recorded on a Shimadzu IR Affinity-1 Fourier transform infrared spectrometer (FTIR) in the 400–4000 cm^{-1} range on the sample that was mixed thoroughly with dried KBr. The Raman spectrum was obtained using a BRUKER RAM II Raman microscope. The spectrum was recorded in the 400–1500 cm^{-1} range.

A second-harmonic generation test was performed on the microcrystalline samples of $Cs_2B_4SiO_9$ by the Kurtz–Perry method. Polycrystalline $Cs_2B_4SiO_9$ was ground and sieved into distinct particle size ranges, <20, 20–38, 38–55, 55–88, 88–105, 105–150, and 150–200 μm. Light of 1064 nm was generated with a Q-switched Nd:YAG solid-state laser. The intensity of the frequency-doubled output emitted from the sample was measured using a photomultiplier tube. Microcrystalline KDP served as the standard and was sieved into the same particle size ranges.

Our calculations employed the CASTEP module as implemented in Material Studio 5.5. The total plane-wave pseudo-potential method forms the basis of the CASTEP calculations. The exchange-correlation effects were treated within the local density approximation (LDA) with the Ceperley and Alder–Perdew–Zunger (CA-PZ) functional. The plane-wave basis set energy cutoff was set at 540.0 eV for $Cs_2B_4SiO_9$, norm-conserving pseudo-potentials were used for all chemical elements. The Monkhorst-Pack scheme k-point grid sampling was set at $4\times3\times2$ for the Brillouin zone. The convergence parameters were as follows: total energy tolerance 2×10^{-6} eV per atom.

Received: November 15, 2012
Revised: January 25, 2013
Published online: February 13, 2013

Keywords: borates · nonlinear optics · solid-state structures · structure–property relationships

[1] C. T. Chen, *Sci. Sin.* **1979**, *22*, 756.
[2] P. Becker, *Adv. Mater.* **1998**, *10*, 979.
[3] D. A. Keszler, A. Akella, K. I. Schaffers, T. Alekel, *Mater. Res. Soc. Symp. Proc.* **1994**, *329*, 15.
[4] H. W. Huang, J. Y. Yao, Z. S. Lin, X. Y. Wang, R. He, W. J. Yao, N. X. Zhai, C. T. Chen, *Angew. Chem.* **2011**, *123*, 9307; *Angew. Chem. Int. Ed.* **2011**, *50*, 9141.
[5] a) C. T. Chen, S. Y. Luo, X. Y. Wang, G. L. Wang, X. H. Wen, H. X. Wu, X. Zhang, Z. Y. Xu, *J. Opt. Soc. Am. B* **2009**, *26*, 1519; b) C. T. Chen, Y. B. Wang, B. C. Wu, K. C. Wu, W. L. Zeng, L. H. Yu, *Nature* **1995**, *373*, 322.
[6] C. T. Chen, B. C. Wu, A. D. Jiang, G. M. You, *Sci. Sin. Ser. B* **1985**, *28*, 235.
[7] C. T. Chen, Y. C. Wu, A. D. Jiang, B. C. Wu, G. M. You, R. K. Li, S. J. Lin, *J. Opt. Soc. Am. B* **1989**, *6*, 616.
[8] C. T. Chen, Z. Y. Xu, D. Q. Deng, J. Zhang, G. K. L. Wong, *Appl. Phys. Lett.* **1996**, *68*, 2930.
[9] C. T. Chen, N. Ye, J. Lin, J. Jiang, W. R. Zeng, B. C. Wu, *Adv. Mater.* **1999**, *11*, 1071.
[10] H. P. Wu, S. L. Pan, K. R. Poeppelmeier, H. Y. Li, D. Z. Jia, Z. H. Chen, X. Y. Fan, Y. Yang, J. M. Rondinelli, H. S. Luo, *J. Am. Chem. Soc.* **2011**, *133*, 7786.
[11] S. F. Jin, G. M. Cai, W. Y. Wang, M. He, S. C. Wang, X. L. Chen, *Angew. Chem.* **2010**, *122*, 5087; *Angew. Chem. Int. Ed.* **2010**, *49*, 4967.
[12] M. D. Donakowski, R. Gautier, J. Yeon, D. T. Moore, J. C. Nino, P. S. Halasyamani, K. R. Poeppelmeier, *J. Am. Chem. Soc.* **2012**, *134*, 7679.
[13] C. F. Sun, C. L. Hu, X. Xu, B. P. Yang, J. G. Mao, *J. Am. Chem. Soc.* **2011**, *133*, 5561.
[14] a) H. S. Ra, K. M. Ok, P. S. Halasyamani, *J. Am. Chem. Soc.* **2003**, *125*, 7764; b) P. S. Halasyamani, K. R. Poeppelmeier, *Chem. Mater.* **1998**, *10*, 2753.
[15] P. Yu, L. J. Zhou, L. Chen, *J. Am. Chem. Soc.* **2012**, *134*, 2227.
[16] T. K. Bera, J. I. Jang, J. B. Ketterson, M. G. Kanatzidis, *J. Am. Chem. Soc.* **2009**, *131*, 75.
[17] J. Jerphagnon, *Phys. Rev. B* **1970**, *2*, 1091.
[18] W. L. Zhang, W. D. Cheng, H. Zhang, L. Geng, C. S. Lin, Z. Z. He, *J. Am. Chem. Soc.* **2010**, *132*, 1508.
[19] Y. Z. Huang, L. M. Wu, X. T. Wu, L. H. Li, L. Chen, Y. F. Zhang, *J. Am. Chem. Soc.* **2010**, *132*, 12788.
[20] M. C. Chen, L. M. Wu, H. Lin, L. J. Zhou, L. Chen, *J. Am. Chem. Soc.* **2012**, *134*, 6508.
[21] K. Kato, *Appl. Phys. Lett.* **1977**, *30*, 583.
[22] Z. G. Hu, M. Yoshimura, Y. Mori, T. Sasaki, *J. Cryst. Growth* **2005**, *275*, 232.

[23] T. K. Bera, J. H. Song, A. J. Freeman, J. I. Jang, J. B. Ketterson, M. G. Kanatzidis, *Angew. Chem.* **2008**, *120*, 7946; *Angew. Chem. Int. Ed.* **2008**, *47*, 7828.
[24] Y. Mori, I. Kuroda, S. Nakajima, T. Sasaki, S. Nakai, *Appl. Phys. Lett.* **1995**, *67*, 1818.
[25] H. W. Yu, H. P. Wu, S. L. Pan, Z. H. Yang, X. Su, F. F. Zhang, *J. Mater. Chem.* **2012**, *22*, 9665.
[26] G. M. Sheldrick, SHELXTL, version 6.14; Bruker Analytical X-ray Instruments, Inc.: Madison, WI, **2003**.
[27] R. K. Li, Y. Yu, *Inorg. Chem.* **2006**, *45*, 6840.
[28] Crystal structure analysis of $Cs_2B_4SiO_9$: MW = 481.15, colorless block, $0.132 \times 0.104 \times 0.072$ mm, tetragonal, space group: $I\bar{4}$, $a = 6.7516(3)$, $c = 9.8906(9)$ Å, Bruker SMART APEX II CCD, Mo radiation ($\lambda = 0.71073$ Å), graphite monochromator, $F(000) = 432$, $\mu = 8.246$ mm, $T = 293(2)$ K; 5175 measured reflections and 1268 independent reflections in the range from 3.65 to 38.49°, $R(\text{int}) = 0.0282$; the data integrate with the SAINT program and refined by a least-square procedure; the final refinement was converged with $R_1 = 0.0362$ and $wR_2 = 0.0776$; the final difference Fourier synthesis map showed the maximum and minimum peaks at 1.82 (0.51 Å from Cs1) and -2.54 e Å^{-3} (0.72 Å from Cs1), respectively; Flack parameter 0.00(4). Further details on the crystal structure investigations may be obtained from the Fachinformationszentrum Karlsruhe, 76344 Eggenstein-Leopoldshafen, Germany (fax: (+49) 7247-808-666; e-mail: crysdata@fiz-karlsruhe.de), on quoting the depository number CSD-425583.
[29] a) S. C. Neumair, J. S. Knyrim, O. Oeckler, R. Glaum, R. Kaindl, R. Stalder, H. Huppertz, *Chem. Eur. J.* **2010**, *16*, 13659; b) E. Zobetz, *Z. Kristallogr.* **1982**, *160*, 81.
[30] a) G. Blasse, G. P. M. van den Heuvel, *Phys. Status Solidi* **1973**, *19*, 111; b) H. W. Yu, S. L. Pan, H. P. Wu, J. Han, X. Y. Dong, Z. X. Zhou, *J. Solid State Chem.* **2011**, *184*, 1644.
[31] a) J. S. Knyrim, F. Roeßer, S. Jakob, D. Johrendt, I. Kinski, R. Glaum, H. Huppertz, *Angew. Chem.* **2007**, *119*, 9256; *Angew. Chem. Int. Ed.* **2007**, *46*, 9097; b) H. Emme, H. Huppertz, *Chem. Eur. J.* **2003**, *9*, 3623; c) J. Zhao, R. K. Li, *Inorg. Chem.* **2012**, *51*, 4568.
[32] a) I. D. Brown, D. Altermatt, *Acta Crystallogr. Sect. B* **1985**, *41*, 244; b) N. E. Brese, M. Okeeffe, *Acta Crystallogr. Sect. B* **1991**, *47*, 192.
[33] a) S. L. Pan, J. P. Smit, B. Watkins, M. R. Marvel, C. L. Stern, K. R. Poeppelmeier, *J. Am. Chem. Soc.* **2006**, *128*, 11631; b) H. P. Wu, S. L. Pan, H. W. Yu, D. Z. Jia, A. M. Chang, H. Y. Li, F. F. Zhang, X. Huang, *CrystEngComm* **2012**, *14*, 799.
[34] S. K. Kurtz, T. T. Perry, *J. Appl. Phys.* **1968**, *39*, 3798.
[35] F. Li, X. L. Hou, S. L. Pan, X. A. Wang, *Chem. Mater.* **2009**, *21*, 2846.
[36] R. K. Li, P. Chen, *Inorg. Chem.* **2010**, *49*, 1561.
[37] a) J. J. Zhang, Z. H. Zhang, Y. X. Sun, C. Q. Zhang, S. J. Zhang, Y. Liu, X. T. Tao, *J. Mater. Chem.* **2012**, *22*, 9921; b) Y. Yang, S. L. Pan, H. Y. Li, J. Han, Z. H. Chen, W. W. Zhao, Z. X. Zhou, *Inorg. Chem.* **2011**, *50*, 2415.
[38] J. Goodey, J. Broussard, P. S. Halasyamani, *Chem. Mater.* **2002**, *14*, 3174.
[39] S. N. Rashkeev, W. R. Lambrecht, *Phys. Rev. B* **2001**, *63*, 165212.
[40] a) S. F. Radaev, B. A. Maximov, V. I. Simonov, B. V. Andreev, V. A. D'yakov, *Acta Crystallogr. Sect. B* **1992**, *48*, 154; b) R. Komatsu, T. Sugawara, N. Watanabe, S. Uda, V. Petrov, *Rev. Laser Eng.* **1999**, *27*, 541; c) J. Krogh-Moe, *Acta Crystallogr. Sect. B* **1974**, *30*, 1178.
[41] a) J. P. Perdew, M. Levy, *Phys. Rev. Lett.* **1983**, *51*, 1884; b) J. Yang, M. Dolg, *J. Phys. Chem. B* **2006**, *110*, 19254; c) Z. S. Lin, L. Kang, T. Zheng, R. He, H. Huang, C. T. Chen, *Comput. Mater. Sci.* **2012**, *60*, 99.
[42] M. H. Lee, C. H. Yang, J. H. Jan, *Phys. Rev. B* **2004**, *70*, 235110.

